Journal of the Physical Society of Japan
Vol. 56, No. 1, January, 1987, pp. 70-78

Elastic Scattering of Electrons from Xenon

Hiroyuki NISHIMURA, Toshiyuki MATSUDA and Atsunori DANJO

Department of Physics, Faculty of Science, Niigata University, 8050 Ikarashi, Niigata 950-21

(Received May 2, 1986)

The differential cross section (DCS) for elastic electron scattering from Xe has been measured using a crossed beam method. The measurements were carried out in the angular range from 10° to 125° and at incident energies from 5 eV to 200 eV. The absolute values of the DCS have been determined by means of the relative flow method. The integral and momentum-transfer cross sections are derived from the measured DCS. The results are compared with those of previous experimental and theoretical studies.

§1. Introduction

Reliable values of electron impact cross sections for heavy atoms are needed in the study of high-power rare-gas excimer lasers, gaseous discharges and electron transportation in gases. In 1931 Bullard and Massey[1] observed diffraction type patterns in the angular distribution of slow electrons elastically scattered from Ar. Since then many theoretical and experimental studies have been carried out on electron-heavy atom collisions.[2] Of particular interest is the fact that the elastic DCS of heavy atoms often exibits a deep narrow minimum at a particular scattering angle,[2,3] and that at that angle spin unpolarized electrons incident on the atoms are partially polarized perpendicularly to the scattering plane after undergoing elastic scattering.

Electron scattering cross sections measured prior to 1978 have been collected and compared with the theoretical predictions in the review article of Bransden and McDowell.[4] Williams and Crowe performed the elastic DCS measurement for Xe (20–400 eV, 20–150°)[5] using a crossed electron beam and modulated atomic beam technique. They determined the absolute values by phase shift analyses of resonant scattering in He and Ar coupled with the determination of the beam density ratios of the relevant target atom to He and Ar. Jansen and de Heer measured the angular distribution of electrons scattered from the static gas Xe target (100–3000 eV, 5–55°).[6] They normalised their values by using the apparatus calibration factors derived from their own absolute measurement of the elastic DCS for N_2. Klewer *et al.* performed the angular distribution measurement of elastic scattering (2–300 eV, 30–120°)[7] and compared their results with the previous experimental and theoretical results. Very recently Register *et al.*[8]* have measured the elastic DCS of Xe (1–100 eV, 10–146°) using a crossed beam technique. They determined the absolute scale by normalizing their relative values of the integral cross section at each energy to the absolute total cross section minus the absolute total ionization and excitation cross sections. They used the total cross sections given by Jost *et al.*[9] and Nickel *et al.*,[10] the total ionization cross section given by de Heer *et al.*,[11] and the total excitation cross section recommended by Hayashi.[12]

Calculations on e-Xe scattering have been carried out by McCarthy *et al.*[13] using the optical model (OM), by Sin Fai Lam[14] using the semi-relativistic method (SR) and by McEachran and Stauffer[15] in the local exchange approximation (LEA). Recently the differential cross section and spin polarization have been calculated by Kemper *et al.*[16] in the relativistic non-local two channel theory (RNL2C).

The total cross section below the excitation

* D. F. Register, L. Vuskovic and S. Trajmar: Submitted to J. Phys. B (1985)

threshold is of course the integral elastic cross section. The measured total cross section is however more reliable than the integral cross section derived from the DCS and so the measured total cross section can be used as an indication of the accuracy of the measured elastic DCS. The total cross section has been measured by Guskov *et al.* (0.025–1 eV),[17] Dababneh *et al.* (0.35–100 eV),[18] (20–800 eV),[19] Wagenaar and de Heer (20–750 eV),[20] Jost *et al.* (0.2–40 eV)[9] and Nickel *et al.* (4–300 eV).[10]

Momentum-transfer cross sections have been measured by Frost and Phelps[21] and by Koizumi *et al.*[22] using a swarm technique. Recommended values have been presented by Hayashi[12] for the total, momentum-transfer and total excitation cross sections by summarizing the recent data.

In spite of all these studies considerable disareements still exist between the measurements and calculations, and also between the experimental results themselves at intermediate impact energies. In particular there is a serious discrepancy concerning the general shape of the angular distribution at 50 eV.

In the present work the elastic e-Xe DCS has been measured in the energy range from 5 eV to 200 eV and in the angular range from 10° to 125°. To minimize the experimental uncertainties we have employed the relative flow method.[23] One aim of the present study is to clarify the validity of the theoretiacl approximations used for electron-heavy atom collisions in the low and intermediate energy regions. The previously reported result[24] is partly refined by the present measurement. The DCS, integral and momentum transfer cross sections are compared with the other experimental and theoretical results.

§2. Experimental Apparatus and Procedures

The electron impact spectrometer and the experimental procedures utilized in the present measurement have been described previously.[25] The Xe beam was effused through a capillary array and crossed at right angles with an electron beam of about 70 meV FWHM. The scattered electrons were energy analyzed and then detected by a channel electron multiplier. The angular resolution of the spectrometer was about ±2°. The true zero scattering angle was determined from the symmetry of the elastic scattering around the nominal zero degree angle. The impact energy scale was calibrated using the elastic scattering resonances at 19.35 eV in He and 7.77 eV in Xe. The magnetic field in the vicinity of the spectrometer was reduced to less than 10 mG by a three dimensional Helmholtz coil and by mu-metal shielding. The procedure for the relative flow method for the determination of the absolute DCS is briefly as follows.[23] The intensity of electrons elastically scattered by Xe was measured and immediately followed by the measurement of the intensity of electrons from He under the same experimental conditions. Thus the intensity ratio of these two target atoms was recorded at each incident energy as a function of scattering angle. Then the absolute value of the elastic DCS for Xe was obtained from this ratio by multiplying it by the absolute DCS for He.[26] The pressure behind the capillary array was adjusted to generate the same flux distribution for the two gases as much as possible.[27] In the present measurement the gas flow system was operated in the pressure range of about 1 torr or lower at the gas reservoir.

For the derivation of the integral and momentum-transfer cross sections it is necessary to extrapolate the measured angular distribution data to 0° and 180°. For this purpose phase shifts are obtained from the measured data and then the angular distribution curve is determined. In the case of a heavy atom target phase shifts should be obtained with a relativistic phase shift analysis.[2] However, at angles where the narrow minimum is not pronounced in the elastic DCS curve, the relativistic effect in the scattering potential is not dominant.[28] Therefore, for the extrapolation of the angular distribution data into the forward and backward angular regions, a non-relativistic phase shift analysis is still useful. The non-relativistic differential cross section is given by (in atomic units);

$$d\sigma/d\Omega = |f(\theta)|^2, \tag{1}$$

$$2ikf(\theta)=\sum_{l=0}^{\infty}(2l+1)[\exp(2i\eta_l)-1]P_l(\cos\theta), \tag{2}$$

where $f(\theta)$ is the scattering amplitude, η_l is the l th phase shift, $P_l(\cos\theta)$ is the l th Legendre polynominal and k is the electron momentum. In principle an infinite number of partial waves should be used. However the first few partial waves are usually dominant and the higher phases can be treated in an approximate way. This leads to the expression;

$$2ikf(\theta)=\sum_{l=0}^{L}(2l+1)[\exp(2i\eta_l)-1]P_l(\cos\theta)+C_L(\theta), \tag{3}$$

$$C_L(\theta)=\pi\alpha k\left\{\frac{1}{3}-\frac{1}{2}\sin(\theta/2)-\sum_{l=1}^{L}P_l(\cos\theta)/(2l+3)(2l-1)\right\}, \tag{4}$$

where α is the atomic polarizability. The DCS is calculated from eqs. (1), (3) and (4) using a trial set of phases and is compared with the experimental angular distributions. The trial set of phases is varied to minimize the χ^2;

$$\chi^2=\frac{1}{N-P-1}\sum_{i=0}^{L}\left\{\frac{x(i)-nX(i)}{\Delta x(i)}\right\}^2, \tag{5}$$

where $x(i)$ is the ith experimental datum with associated error $\Delta x(i)$, $X(i)$ is the corresponding value calculated from the trial set, N is the number of experimental points and P is the number of phases to be varied. The normalization factor n is also treated as an adjustable parameter. In the present analysis 5 to 10 phases were varied.

The uncertainties in the counting statistics were negligibly small except at scattering angles near the minima in the DCS curve at high impact energies, where they were about

Table I. Elastic differential scattering cross sections (Å^2 sr^{-1}).

θ(deg) \ E_0(eV)	5.0	6.0	8.0	10.0	12.0	15.0	17.5	20.0	25.0	30.0
10	—	—	—	—	—	42.8	39.8	45.1	27.6	18.2
15	11.9	21.7	—	—	26.3	31.1	34.8	32.3	21.4	12.7
20	10.3	17.1	16.9	17.4	19.6	24.3	24.0	24.7	16.2	8.22
30	5.91	10.4	10.4	13.1	11.3	13.7	12.6	10.0	6.71	3.29
40	3.98	5.80	7.23	6.88	5.88	6.17	4.49	3.04	1.21	0.777
45	—	—	—	—	—	—	—	—	0.312	0.333
50	2.73	3.52	3.65	3.71	2.75	2.32	1.31	0.462	0.0614	0.153
55	—	—	—	—	—	1.44	0.734	0.199	0.0750	0.172
60	2.53	2.40	2.26	1.96	1.31	0.996	0.531	0.308	0.286	0.294
62	—	—	—	—	—	—	0.522	—	—	—
65	—	—	—	—	—	—	0.583	—	0.550	—
70	2.61	2.07	1.38	1.25	0.813	0.619	0.617	0.617	0.704	0.459
75	—	—	—	—	—	—	—	—	0.703	—
80	2.31	1.72	1.32	0.929	0.600	0.483	0.528	0.595	0.537	0.331
90	2.18	1.68	1.31	0.750	0.478	0.425	0.399	0.293	0.208	0.144
95	—	—	1.15	—	—	0.404	0.315	0.149	0.0702	0.110
100	1.12	0.863	0.943	0.690	0.456	0.397	0.252	0.0955	0.0352	0.161
105	—	0.549	0.655	0.537	—	—	0.324	0.0987	—	0.250
110	0.185	0.283	0.489	0.500	0.485	0.495	0.386	0.159	0.160	0.330
115	0.0371	0.122	—	0.520	—	—	—	—	0.177	0.359
120	0.0983	0.211	0.312	0.550	0.524	0.644	0.518	0.253	0.160	0.346
125	0.390	0.544	—	—	0.585	0.636	0.535	0.244	0.152	0.253
σ_I(Å^2)	33.9	44.4	41.3	37.8	34.1	39.8	35.3	29.5	18.9	12.6
σ_M(Å^2)	24.9	29.9	24.5	16.8	10.4	9.02	7.21	5.65	3.59	5.04

5%. The estimated error due to the change of the incident electron current and its intensity profile is about 10%. The pressure ratio was determined within a 5% uncertainty. Another error in the determination of the DCS is due to the limited angular resolution of the spectrometer. This error is estimated to be 10% in the angular region of forward scattering and near minima. Taking into account the accuracy of the standard elastic DCS for He[26] the combined uncertainty of the present elastic DCS is about 17%. For the integral and momentum-transfer cross sections, an additional error is introduced due to the extrapolation of the measured DCS to 0° and 180°. This uncertainty is estimated to be 15–20%.

§3. Results and Discussion

The absolute values of the DCS obtained in the present measurement are listed in Table I. Integral and momentum-transfer cross sections derived by extrapolating the data to 0° and 180° are also given in Table I. The phase shifts obtained by fitting eqs. (1)–(5) to the measured angular distribution data are tabulated in Table II. These values are in reasonably good agreement with the phase shifts obtained by the RNL2C calculation of

Table I. continued

E_0(eV) / θ(deg)	40.0	50.0	60.0	70.0	80.0	100.0	120.0	150.0	200.0
10	17.4	13.4	15.5	14.2	12.6	12.5	10.8	8.28	8.40
15	9.93	7.28	6.52	5.86	5.10	4.18	3.98	2.94	3.17
20	5.26	3.17	2.52	1.97	1.67	1.15	1.13	0.740	0.814
25	—	—	—	—	0.255	0.173	0.311	0.251	0.542
27	—	—	—	—	—	0.133	—	—	—
28	—	—	—	—	0.0797	—	—	—	—
30	1.34	0.461	0.173	0.0579	0.0550	0.105	0.237	0.326	0.452
34	—	—	—	0.0413	—	—	—	—	—
35	—	—	0.0700	—	0.128	0.266	0.316	0.420	0.468
40	0.278	0.0565	0.0672	0.105	0.229	0.337	0.430	0.419	0.325
45	—	—	0.0896	0.145	—	0.328	0.388	0.317	—
50	0.0505	0.0104	0.0715	0.134	0.208	0.258	0.295	0.192	0.0867
53	0.0400	—	—	—	—	—	—	—	—
55	0.053	0.00394	—	—	—	0.142	—	0.0706	0.0281
57	—	0.0102	—	—	—	—	—	—	—
60	0.0751	0.0157	0.0195	0.0361	0.0593	0.0603	0.0410	0.00619	0.00825
65	—	—	0.0111	—	0.0137	0.0104	0.00465	0.0158	—
66	—	—	—	—	—	0.00929	—	—	—
67	—	—	—	—	—	0.00986	—	—	—
70	0.126	0.0359	0.00815	0.00297	0.00878	0.0221	0.0342	0.0655	0.107
75	—	—	0.0103	—	0.0237	0.0679	—	0.145	0.190
80	0.108	0.0317	0.00761	0.0143	0.0529	0.104	0.153	0.189	0.225
85	0.0856	0.0288	0.00339	0.0175	0.0592	0.153	—	—	—
87	0.0758	—	—	—	—	—	—	—	—
88	—	—	0.00364	—	—	—	—	—	—
90	0.105	0.0357	0.00553	0.0157	0.0515	0.144	0.172	0.183	0.178
92	—	—	—	0.0178	—	—	—	—	—
95	—	—	—	—	0.0434	0.117	0.153	—	—
100	0.239	0.119	0.0663	0.0404	0.0471	0.0868	0.0795	0.0665	0.0385
105	—	—	—	—	0.0574	0.0518	—	0.0236	0.00900
110	0.393	0.299	0.193	0.139	0.0873	0.0362	0.0194	0.00145	0.0180
115	—	—	—	—	0.101	0.0415	0.0139	0.00981	—
120	0.392	0.378	0.271	0.200	0.150	0.0498	0.0222	0.0316	0.0956
125	0.291	0.338	0.265	0.184	—	0.0562	0.0352	0.0544	0.117
σ_I(Å^2)	9.87	6.96	6.54	5.61	4.79	4.56	4.55	3.89	3.68
σ_M(Å^2)	5.07	3.15	2.25	1.90	1.12	1.39	1.68	1.19	1.28

Table II. Summary of phase shifts (rad)

E_0(eV)	$L=0$	$L=1$	$L=2$	$L=3$	$L=4$	$L=5$	$L=6$	$L=7$	$L=8$	$L=9$
5.0	2.136	2.528	0.814	−2.989	0.003	—	—	—	—	—
6.0	2.027	2.632	1.252	−2.863	0.074	0.070	0.012	—	—	—
8.0	1.964	2.467	1.372	−2.882	0.076	—	—	—	—	—
10.0	1.775	2.244	1.369	−2.784	0.094	—	—	—	—	—
12.0	1.589	1.994	1.398	−2.604	0.130	—	—	—	—	—
15.0	1.296	1.804	1.361	−2.392	0.188	0.108	—	—	—	—
17.5	1.260	1.664	1.440	−2.141	0.206	0.083	—	—	—	—
20.0	0.891	1.437	1.106	−2.178	0.216	0.100	0.075	0.040	—	—
25.0	1.005	1.205	1.321	−1.831	0.355	—	—	—	—	—
30.0	1.049	1.218	0.901	−1.496	0.123	0.150	0.207	—	—	—
40.0	0.508	0.530	0.891	−0.054	0.365	0.198	—	—	—	—
50.0	0.143	0.570	0.778	0.017	0.493	0.226	—	—	—	—
60.0	−0.018	0.402	0.521	0.069	0.476	0.240	—	—	—	—
70.0	−0.090	0.404	0.570	0.120	0.642	0.314	—	—	—	—
80.0	−0.526	0.349	0.474	0.276	0.690	0.405	—	—	—	—
100.0	−0.866	0.188	0.513	0.328	1.057	0.516	0.321	0.203	0.144	0.128
120.0	−1.113	−0.086	0.593	0.294	1.148	0.531	0.398	0.182	0.145	0.113
150.0	−1.184	−0.023	0.360	0.435	1.596	0.860	0.558	0.343	0.232	0.196
200.0	−1.353	−0.900	0.418	0.107	1.302	0.692	—	—	—	—

Kemper *et al.*

The present DCS values at 5, 10, 50, 100 and 200 eV are shown in Figs. 1–5 respectively, along with the previous experimental and theoretical results. The dominant features of the angular distribution are the 'diffraction pattern' type maxima and minima.

At the lowest energies (5–8 eV) a shallow minimum and a sharp minimum are observed in the mesured DCS (Fig. 1). The recent experimental results of Register *et al.*[8] in the same energy region (4.75 eV and 5.75 eV) are

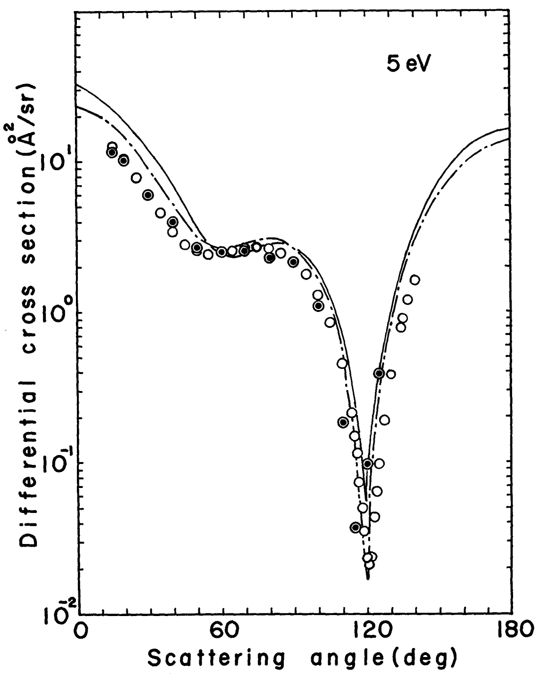

Fig. 1. Differential cross sections at 5 eV. Experiment: ◉: present results, ○: Register *et al.* at 4.75 eV. Calculation: —·—: Sin Fai Lam, ——: McEachran and Stauffer.

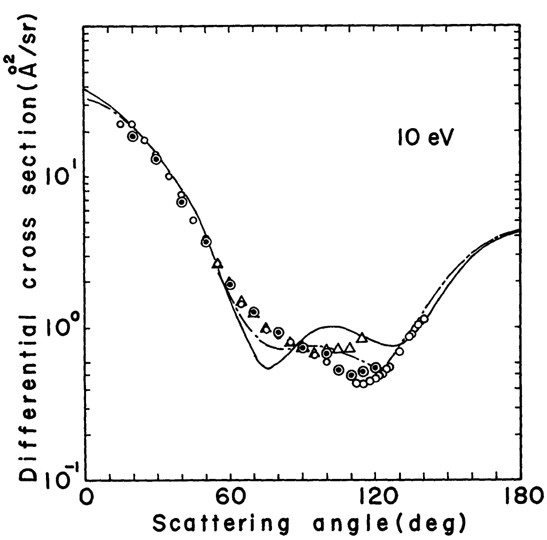

Fig. 2. Differential cross sections at 10 eV. Experiment: ◉: present results, ○: Register *et al.* at 9.75 eV, △: Klewer *et al.* (normalized to the present data at 90°). Calculation: —·—: Sin Fai Lam, ——: McEachran and Stauffer.

in good agreement with the present measurements except for a small difference in the position of the minimum near 120°C. This angular discrepancy may arise partly from the difference in impact energies studied. The theoretical results of McEachran and Stauffer have essentially the same shape of angular distribution but have a significantly different magnitude. This discrepancy in the DCS has been considerably improved by Sin Fai Lam. In the energy region 10–12 eV the measured angular distribution data show a smooth decrease with increasing scattering angle except for a tendency to increase at backward scattering angles. As can be seen in Fig. 2, the present measurements are in excellent agreement with those of Register *et al.* at 10 eV. The result of Klewer *et al.*, which is normalized to the present result at 90°C, is also in excellent agreement except at the backward scattering angles. There is a good agreement both in shape and magnitude between the present results and those calculated by McEachran and Stauffer and by Sin Fai Lam at forward and backward scattering angles. The discrepancy between the experimental and the theoretical results at intermediate scattering angles has been reduced by Sin Fai Lam. In the present measurements distinct minima and maxima have begun to grow at 15 eV. There is an excellent agreement between the present results and those of Register *et al.* at the commonly measured energies (Figs. 3–5). There is good agreement between the present DCS data and those of Williams and Crowe in the forward angular region at 20 and 60 eV, in the backward angular region at 30 eV and for all angles at 200 eV. The agreement between the present results and those of Jansen and de Heer at 100, 150 and 200 eV is also excellent.

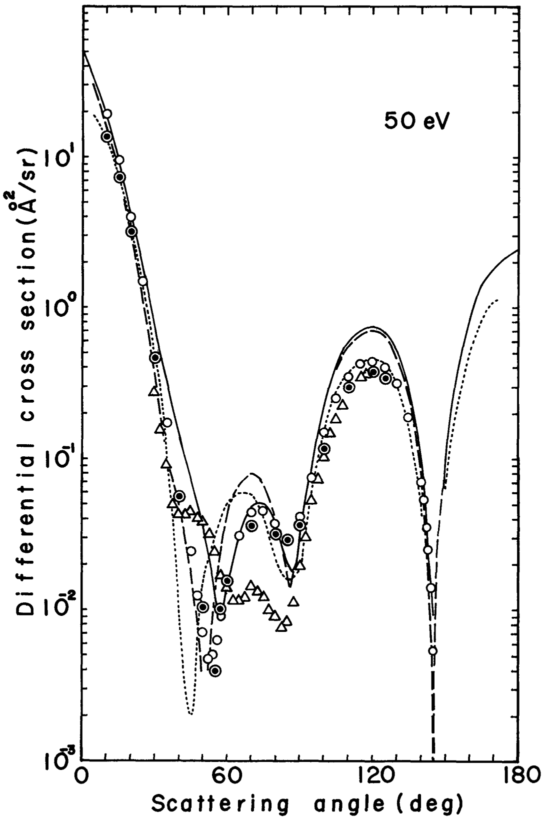

Fig. 3. Differential cross sections at 50 eV. Experiment: ◉: present results, ○: Register *et al.* at 49.75 eV, △ Klewer *et al.* (normalized to the present data at 120°). Calculation: ······: McCarthy *et al.*, ——: McEachran and Stauffer, — —: Kemper *et al.*

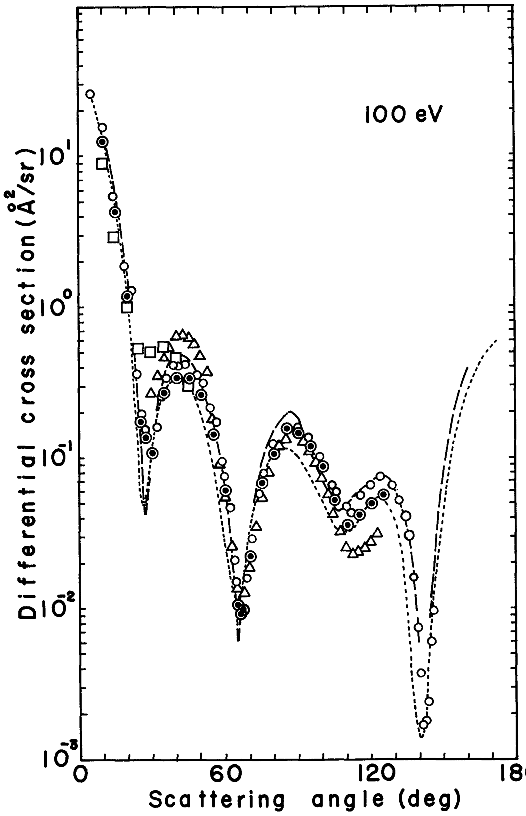

Fig. 4. Differential cross sections at 100 eV. Experiment: ◉: present results, ○: Register *et al.*, □: Jansen and de Heer, △: Klewer *et al.* (normalized to the present data at 80°). Calculation: ······: McCarthy *et al.*, ——: McEachran and Stauffer.

At 50 eV the earlier result of Klewer *et al.*[7] (normalized at 120° to the present result) gives a completely different angular distribution in the angular region between 40° and 90° (Fig. 3). Since the angular distribution of Klewer *et al.*[7] at 50 eV is similar to the present result at 60 eV, the discrepancy may be attributable to an inaccuracy in their impact energy.

The calculation of McEachran and Stauffer[15] in LEA reproduces the shape of the present DCS results at 5(Fig. 1), 25, 30, and 50 eV, and both the shape and magnitude at 10 eV(Fig. 2). The theoretical result of Sin Fai Lam in SR is nearly the same as that of McEachran and Stauffer at 5 eV(Fig. 1) and 10 eV(Fig. 2). A noticeable discrepancy in magnitude is found between the present results and those of Sin Fai Lam with increasing impact energy. The calculations of McEachran and Stauffer[15] in LEA and of Sin Fai Lam[14] in SR predict the present results reasonably well at lower impact energies. The theoretical results of McCarthy *et al.*[13] in OM reproduce the present results very well except at 30 and 50 eV(Fig. 3). The calculations of Kemper *et al.*[16] in RNL2C follow the present results very well in the higher energy region (Figs. 4 and 5). At 50 eV, the agreement is reasonably good except at the angles from 40° to 90° (Fig. 3). At lower energies (25, 30 eV), their theoretical prediction is not so good as far as the magnitude is concerned.

In Fig. 6 the integral cross section (σ_I) derived from the measured DCS is shown together with the experimental results of Register *et al.*[8] (derived from the DCS) and Nickel *et al.*[10] (total cross section measurement), and the calculations of McCarthy *et al.*[13] (obtained from the numerical integration of their DCS values by the present authors), McEachran and Stauffer,[15] and Sin Fai Lam.[14] The cross section curve has a broad maximum at low energies(6–15 eV), after which it gradually decreases up to 70 eV. Above 70 eV the cross section is nearly constant with impact energy. The agreement between the two DCS measurements is very good except for a small discrepancy at higher impact energies. This discrepancy may be partly attributed to the different procedures used for obtaining the absolute DCS values. There is excellent agreement between the integral cross section der-

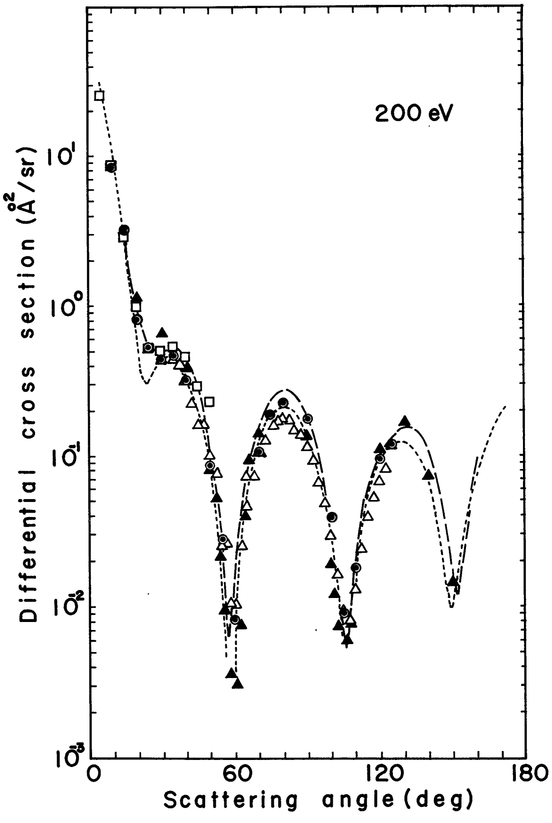

Fig. 5. Differential cross sections at 200 eV. Experiment: ◉: present results, ▲: Williams and Crowe, △: Klewer *et al.* (normalized to the present data at 80°), Calculation: ······: McCarthy *et al.*, — —: Kemper *et al.*

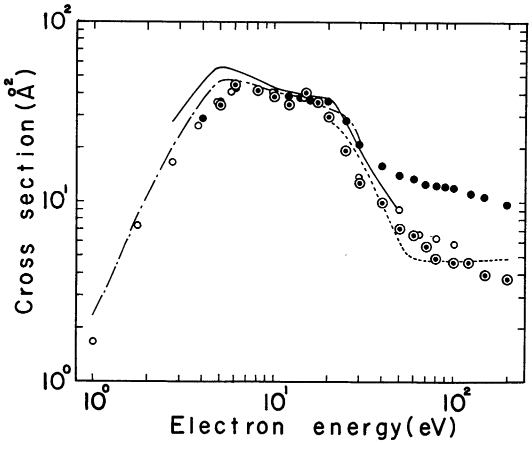

Fig. 6. Integral cross sections for elastic scattering. Experiment: ◉: present results, ○: Register *et al.*, ●: Nickel *et al.* (total cross section). Calculation: ······: McCarthy *et al.*, —·—: Sin Fai Lam, ——: McEachran and Stauffer.

ived from the DCS and the measured total cross section at energies below the excitation threshold. The calculation of McEachran and Stauffer[15] shows fairly good agreement with the experimental results except at lower energies. The result of Sin Fai Lam[14] is in reasonably good agreement with the experimental results at energies up to 20 eV. At higher energies his values are considerably higher than the present values. The agreement between the present result and that of McCarthy *et al.*[13] is very good in the energy region of overlap.

The elastic momentum transfer cross section (σ_M) derived from the measured DCS is shown in Fig. 7 together with those of previous experiments and calculations. The present result agrees well with that of Register *et al.*[8] The swarm experiment of Frost and Phelps[21] shows reasonably good agreement with the results of the beam experiments at energies lower than 6 eV. At higher energies there is a significant disagreement between these two types of experiment. The recent swarm experiment of Koizumi *et al.*[22] gives higher values than those obtained by Frost and Phelps. The theoretical result of McEachran and Stauffer[15] shows considerably higher values in the lower energy region and at energies around 30 eV. The present result is in good agreement with that of Sin Fai Lam[14] in the energy range up to 20 eV. The calculation of McCarthy *et al.*[13] again reproduces the present result very well at the energies compared.

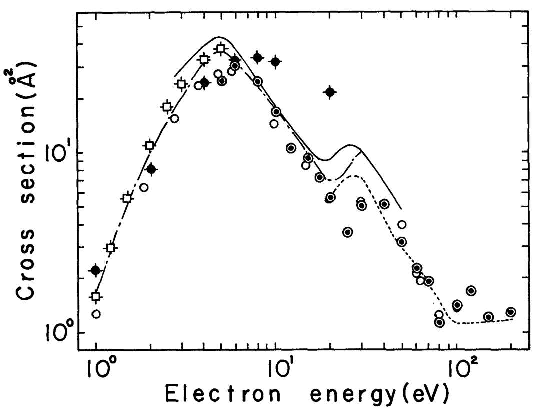

Fig. 7. Momentum transfer cross sections. Experiment: ◉: present results, ○: Register *et al.*, ✦: Frost and Phelps (swarm), ✧: Koizumi *et al.* (swarm). Calculation: ------: McCarthy *et al.*, —·—: Sin Fai Lam, ——: McEachran and Stauffer.

§4. Concluding Remarks

The present cross sections (DCS, σ_I, σ_M) agree very well with the recent results of Register *et al.*[8] throughout the impact energies observed. The previous experimental DCS data of Williams and Crowe[5] and those of Jansen and de Heer[6] show good agreement both in shape and magnitude with the present result at high impact energies, but substantial differences exist in magnitude at certain angles in the low impact energy region. The theoretical calculations of McCarthy *et al.*[13] in OM and Kemper *et al.*[16] in RNL2C reproduce the present cross section well except at around 50 eV, where they fail to reproduce the measured angular distribution from 40° to 90°. At lower energies (up to 20 eV), on the other hand, the calculated results (DCS, σ_I, σ_M) of Sin Fai Lam[14] in SR predict the present result reasonably well. Throughout this work, the usefulness of the relative flow method has been demonstrated.

Acknowledgements

We would like to express our gratitude to Dr. S. Trajmar for supplying us their results prior to publication. We are greatly indebted to Professors K. Takayanagi and F. H. Read for their critical reading of the typescript.

References

1) E. C. Bullard and H. S. W. Massey: Proc. R. Soc. London **A130** (1931) 579.
2) H. S. W. Massey and E. H. S. Burhop: *Electronic and Ionic Impact Phenomena* (Oxford University Press (Clarendon), London and New York, 1969) Vol. 1.
3) J. Kessler: *Polarized Electrons* (Springer, Berlin, Heidelberg and New York, 1976).
4) B. H. Bransden and M. R. C. McDowell: Phys. Rep. **46** (1978) 249.
5) J. F. Williams and A. Crowe: J. Phys. **B8** (1975) 2233.
6) R. H. J. Jansen and F. J. de Heer: J. Phys. **B9** (1976) 213.
7) M. Klewer, M. J. M. Beerlag and M. J. van der Wiel: J. Phys. **B12** (1979) 3935.
8) D. F. Register, L. Vuskovic and S. Trajmar: submitted to J. Phys. B (1985) and private communication (1985).
9) K. Jost, P. G. F. Bisling, F. Eschen, M. Felsmann and L. Walther: *Proc. 13th Int. Conf. the Physics of*

Electronic and Atomic Collisions, Berlin 1983, ed. J. Eichler, W. Fritsch, I. V. Hertel, N. Stollerfoht and U. Wille (North Holland, Amsterdam) Abstract p. 91.

10) J. C. Nickel, K. Imre, D. F. Register and S. Trajmar: J. Phys. B**18** (1985) 125.
11) F. J. de Heer, R. H. J. Jansen and W. van der Kaay: J. Phys. B**12** (1979) 979.
12) M. Hayashi: J. Phys. D**16** (1983) 581.
13) I. R. McCarthy, C. J. Noble, B. A. Phillips and H. D. Turnbull: Phys. Rev. A**15** (1977) 2173.
14) L. T. Sin Fai Lam: J. Phys. B**15** (1982) 119.
15) R. P. McEachran and A. D. Stauffer: J. Phys. B**17** (1984) 2507.
16) F. Kemper, F. Rosickey and R. Feder: J. Phys. B**18** (1985) 1223.
17) Y. Y. Guskov, R. V. Savvov and V. A. Slobodyanynk: Sov. Phys.-Tech. Phys. **23** (1978) 167.
18) M. S. Dababneh, W. E. Kauppila, J. P. Dowring, F. Laperriere, V. Pol, J. H. Smart and T. S. Stein: Phys. Rev. A**22** (1980) 1872.
19) M. S. Dababneh, Y. F. Hsieh, W. E. Kauppila, V. Pol and S. Stein: Phys. Rev. A**26** (1982) 1252.
20) R. W. Wagenaar and F. J. de Heer: J. Phys. B **13** (1980) 3855.
21) L. S. Frost and A. V. Phelps: Phys. Rev. **136** (1964) A1538.
22) T. Koizumi, E. Shirakawa and I. Ogawa: RUP 85-5 (Rikkyo Univ. (preprint)).
23) S. K. Srivastava, A. Chutjian and S. Trajmar: J. Chem. Phys. **63** (1975) 2659.
24) H. Nishimura, A. Danjo and T. Matsuda: *Proc. 14th Int. Conf. on the Physics of Electronic and Atomic Collisions, Palo Alto, 1985*, ed. M. J. Coggiola, D. L. Huestis and R. P. Saxon, Abstracts p. 108.
25) H. Nishimura, A. Danjo and H. Sugahara: J. Phys. Soc. Jpn. **54** (1985) 1757.
26) D. F. Register, S. Trajmar and S. K. Srivastave: Phys. Rev. A**21** (1980) 1134.
27) S. Trajmar and D. F. Register: *Electron-Molecule Collisions*, ed. I. Shimamura and K. Takayanagi (Plenum, New York and London, 1983).
28) D. W. Walker: Adv. Phys. **20** (1971) 257.